Applied Physics Research; Vol. 15, No. 2; 2023
ISSN 1916-9639 E-ISSN 1916-9647
Published by Canadian Center of Science and Education

Applied Physics of Extended (or Gamma) Sine and Cosine Functions

Luis Teia[1]

[1] von Karman Institute for Fluid Dynamics, Chaussée de Waterloo 72, 1640 Rhode-Saint-Genèse, Belgium

Correspondence: Dr Luis Teia, von Karman Institute for Fluid Dynamics, Chaussée de Waterloo 72, 1640 Rhode-Saint-Genèse, Belgium. E-mail: luisteia@sapo.pt

Received: April 10, 2023 Accepted: May 17, 2023 Online Published: July 25, 2023

doi:10.5539/apr.v15n2p1 URL: https://doi.org/10.5539/apr.v15n2p1

Abstract

Evolution of fundamental mathematical tools (such as trigonometric functions $\sin(\alpha)$ and $\cos(\alpha)$) has inherent repercussions on how we solve problems in applied physics. Recently published extended or gamma sine function $\sin^*(\alpha, \gamma)$ and cosine function $\cos^*(\alpha, \gamma)$ — along with their upgraded identity angle sum and subtraction rules $\sin^*(A \pm B, \gamma)$ and $\cos^*(A \pm B, \gamma)$ — have enabled a new approach on how to tackle practical problems using mathematics (a published example is the energy-coupled mass-spring oscilatory system). The usefullness of a theory is measured by both the insight it generates, and the solution it produces, when applied to physical problems with pertinent applications. Its acceptance amongst peers depends on the availability of such examples, as way-showers of how the theory can be applied in practice, and how useful results can be derived by employing it in similar or related examples/problems. This article has the purpose of providing this bridge between the above theories and its application in some common scientific fields. Several exercises are solved employing these new formulae, and new potential applications are identified that cover various topics in physics such as civil engineering (i.e., measuring distances in bridges), aerospace and aeronautics (i.e., turbine velocity triangles and optimum orbital deployment for a satellite constellation) and telecommunications (i.e., antenna array beamforming and steering, as well as new modulations based on quadrature phase-shift keying). These problems (and solutions) are designed to indicate the usefullness of these new expanded functions, and can become practical classroom exercises applicable to both academic and professional environments.

Keywords: gamma, trigonometry, applied, physics, exercises

Ever since sailors aligned quadrants with stars to guide themselves through the perils of the oceans, the need to project angles into distances (and vice versa) has been an inevitability for humanity in its endeavor for territorial and technological expansion. In modern times, this need still exists and is again present during the navigation of the SpaceX Dragon "Axiom-1" capsule as it made its final approach (with its four astronauts) into the International Space Station on April 9^{th}, 2022. Trigonometric functions such as $\sin(\alpha)$ and $\cos(\alpha)$ are tools used to determine side lengths of a right triangle resulting from the orthogonal projection of the hypotenuse about a given internal reference angle α. Being inherently connected to the Pythagoras theorem, they only function encompassed in right-angle triangles (or in triangles where one of its internal angles is $\gamma = 90$ degrees). If the internal angle changes to $\gamma = 120$ degrees, what would these functions look like (Figure 1)? The projected lengths of the hypotenuse given by the traditional sine and cosine would change — this time dependent on both angles α and γ — or simply put, into $\sin^*(\alpha, \gamma)$ and $\cos^*(\alpha, \gamma)$ [where the asterisk sign * implies that they are different from the original sine and cosine]. A typical approach to finding the side lengths and angles of a scalene triangle is to subdivide it into two right triangles and employ trigonometric operations. The resorting to orthogonality to solve a non-orthogonal problem is not an organic approach, and a more direct trigonometric and mathematical path is desired. If a mathematician or scientist is faced with a problem where he/she needs to know the (normalized) sides of a scalene triangle based on its angles, then the functions $\sin(\alpha)$ and $\cos(\alpha)$ [valid only for right triangles] need to be replaced by more generic expressions, herein termed the *gamma or extended sine and cosine functions* — denoted as $\sin^*(\alpha, \gamma)$ and $\cos^*(\alpha, \gamma)$, respectively.

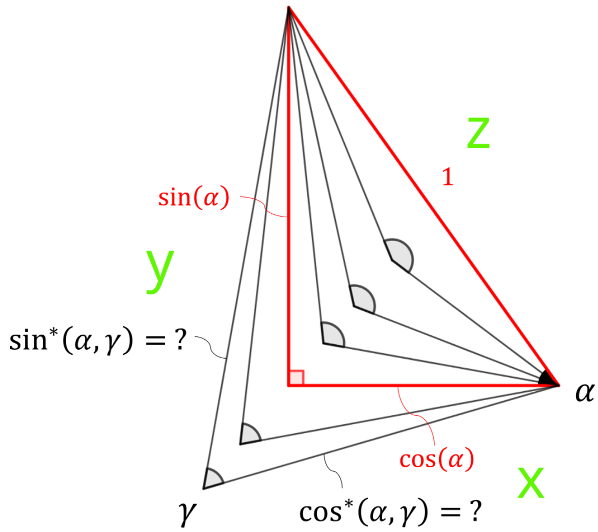

Figure 1. Extending the notion of sine and cosine functions into scalene triangles (Teia 2022c)

These functions and rules fall within the domain of non-orthogonal or *gamma trigonometry*. They expand the usefulness of application of the already existing trigonometric functions in a variety of scientific fields, ranging from orbital mechanics (Curtis, 2010), electronics (Rawlins, 2000), chemistry (Howard, 2018) and design (Parisher, 2012). Both the Pythagoras' theorem and trigonometry (in general) form part of most secondary education curricula around the world, including in the American, Canadian and Australian Curriculum (Reys 2007, Canadian Ministry of Education 2020, Australian Curriculum n.d.), which makes this paper of interest to both students and professionals.

1. Hypothesis

It is the hypothesis of this study that generalization of fundamental trigonometric functions should enable both a new understanding of, and a new way of solving advanced physical problems (dependent on trigonometric relations), such as those found in civil engineering, aerospace & aeronautic and telecommunications.

2. Theory

Gamma trigonometry is a new field of mathematics that expands classical trigonometric functions from an orthogonal environment (i.e., the common axes system are at right-angles or $\gamma = 90$ deg) into a non-orthogonal or oblique environment (i.e., the system axes are at any angle to each other or $\gamma \neq 90$ deg) [Teia 2021a-2023]. The Law of Cosines [Eq.(1)] is a broad expression that relates the lengths of the three sides x, y and z of any triangle (Maor 2007, Pickover 2012), which not only covers the particular case of the Pythagoras theorem $x^2 + y^2 = z^2$ (where orthogonality defines the internal reference angle as $\gamma = \pi/2$ possible values of γ that result in angle and distance relation within a scalene triangle.

$$z^2 = y^2 + x^2 - 2xy\cos(\gamma) \tag{1}$$

The particular case of the Pythagoras theorem is satisfied by replacing $\gamma = 90$ deg, $x = \cos(\alpha)$, $y = \sin(\alpha)$ and $z = 1$. Similarly, it was proven in (Teia, 2021c) that the general case of the Law of Cosines is fulfilled by the extended expressions (defined below), implying a scalene triangle with sides x, y and z (as in Figure 1). It was further proven that the expressions for the extended (or also called gamma) sine function $\sin^*(\alpha, \gamma)$ and cosine function $\cos^*(\alpha, \gamma)$ applicable to scalene triangles (Figure 1) [where the extended hypotenuse is normalized (i.e., $z = 1$)] are given as

$$y = \sin^*(\alpha, \gamma) = \frac{\sin(\alpha)}{\sin(\gamma)} \tag{2}$$

$$x = \cos^*(\alpha, \gamma) = \cos(\alpha) + \frac{\sin(\alpha)}{\sin(\gamma)}\sin(\alpha) = \frac{\sin(\alpha + \gamma)}{\sin(\gamma)} \tag{3}$$

In trigonometry, the angle sum and difference identity rules establish a link between additive or subtractive operations in angles with its impact on the lengths of their respective right triangles, and are commonly defined as

$$\sin(A \pm B) = \sin(A)\cos(B) \pm \cos(A)\sin(B) \tag{4}$$

$$\cos(A \pm B) = \cos(A)\cos(B) \mp \sin(A)\sin(B) \tag{5}$$

This is only applicable to a triangle with an obtuse angle $\gamma = 90$ deg — i.e. a right-angled triangle. In a recent publication (Teia, 2022d), the definition of these rules has been extended to encompass scalene triangles, which accommodate a broader application including scalene triangles with any obtuse angle. For the summing of angles of the identity rule (where $\alpha = A + B$)[Figure 2a], these were proven to be

$$\sin^*(A + B, \gamma) = \sin^*(A, \gamma)\cos^*(B, \gamma) + \cos^*(A, \pi - \gamma)\sin^*(B, \gamma) \tag{6}$$

$$\cos^*(A + B, \gamma) = \cos^*(A, \gamma)\cos^*(B, \gamma) - \sin^*(A, \pi - \gamma)\sin^*(B, \gamma) \tag{7}$$

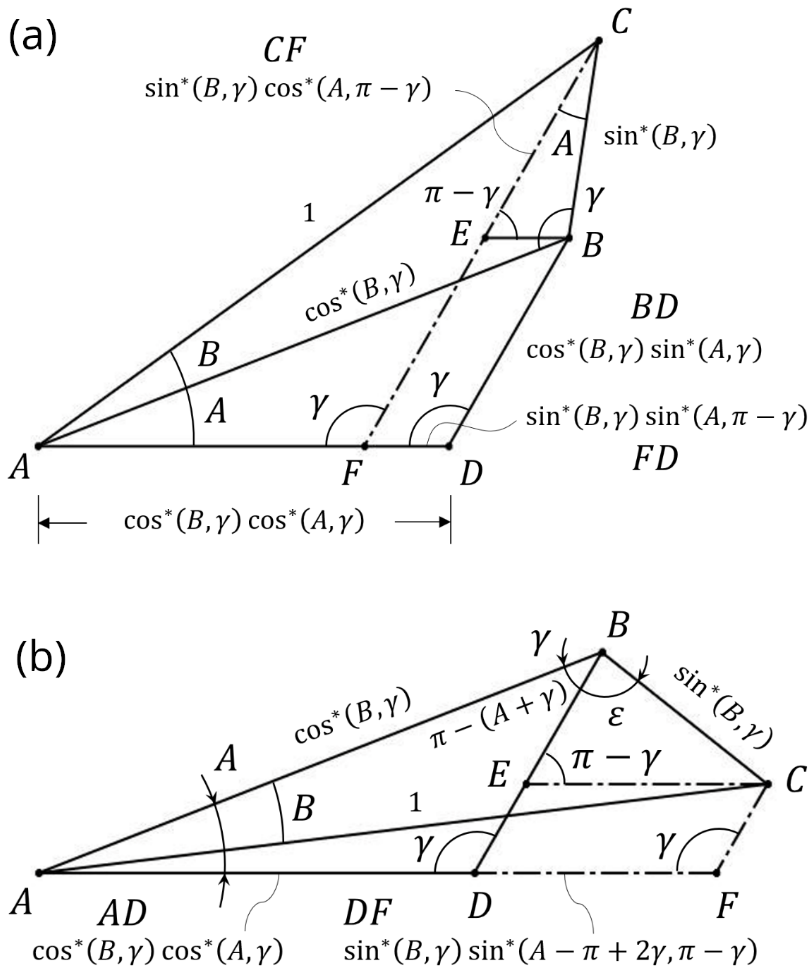

Figure 2. An angle (a) summation and (b) subtraction within a scalene triangle and associated projections [11]

For the angle difference identity rule (where $\alpha = A - B$)[Figure 2b], these were proven to be

$$\sin^*(A - B, \gamma) = \sin^*(A, \gamma)\cos^*(B, \gamma) - \cos^*(A - \pi + 2\gamma, \pi - \gamma)\sin^*(B, \gamma) \tag{8}$$

$$\cos^*(A - B, \gamma) = \cos^*(A, \gamma)\cos^*(B, \gamma) + \sin^*(A - \pi + 2\gamma, \pi - \gamma)\sin^*(B, \gamma) \tag{9}$$

Note that Figure 2a and 2b are practically the same, except that the scalene triangle $\triangle ABC$ is upwards in Figure 2a (adding angle B to A), and it is downwards in Figure 2b (subtracting angle B from A). This article focuses on the application of these equations; further details on their proofs can be found in the respective publication (Teia 2022c, Teia 2022d).

3. Exercises & Possibilities

There are several domains in physics that require classical (orthogonal, i.e., sine and cosine functions assume with $\gamma = 90$ deg) trigonometry to solve. The point of this article is to solve equivalent problems that fall beyond orthogonality, requiring the extended sine and cosine functions — i.e., Eq.(2-3) — and their identity rules — i.e., Eq.(6-9)— which have a broad application to scalene triangles, much in the same manner as conventional sine and cosine functions are applicable to right triangles (hence enabling a scientist or mathematician the possibility to, when the orthogonal condition fails, to replace the conventional sine and cosine by their extended versions immediately and effortlessly — culminating in a more flexible mathematical solution). Moreover, the new extended trigonometric functions open doors for possibilities of expanding scientific fields in which they (the functions) are the foundations. Some possibilities will be presented and discussed briefly. Exercises are marked as (E) while possibilities are marked as (P). In order to assist the confirmation of the solutions of the following gamma trigonometric problems, the open-source program Geogebra (Feng, 2013) can be used to draw the involved scalene triangles, as well as, in determining their lengths and angles.

4. Civil Engineering

4.1 Inclined Bridge (E)

Problem. A suspension bridge has a series of main suspension cables connecting the horizontal road deck (through which the automobiles transit) to the vertical tower, making an angle $\gamma = 90$ deg (Figure 3). The main suspension cables transmit tension forces and connect from anchors (i.e., concrete blocks at shore — located out of the photo to the left beyond point A) at each of their ends to the top of the intermediate towers (Pipinato, 2021). The two connection points A and B have an original average diagonal cable length of 2km, where the cables are not completely stretched, making an angle of $\alpha = 30$ degrees with the horizontal. Over the years, the foundations yielded and the tip of the tower at point B is now a half a degree inclined in the direction away from the cables (the change of inclination from B to B' was measured at point C by an engineer with a theodolite). How much have the cables stretched due to the inclination?

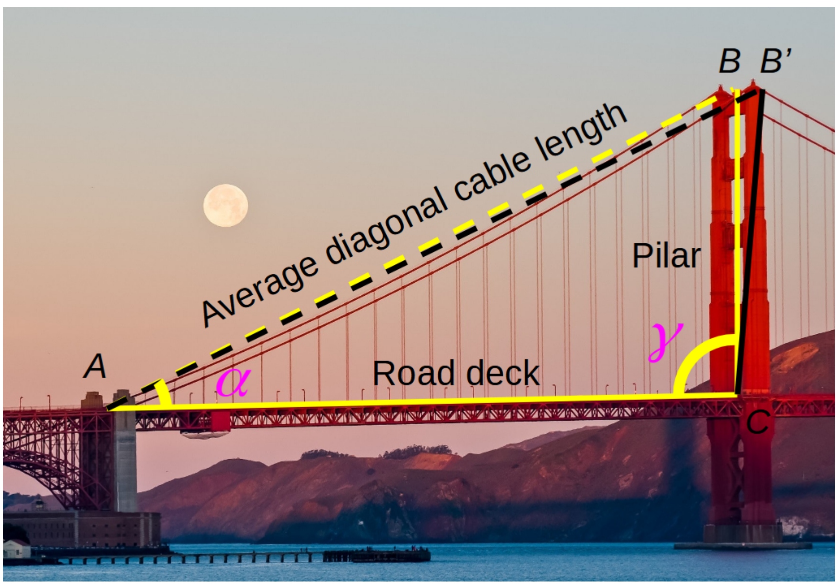

Figure 3. Assessment in a suspension bridge of cable elongation due to inclination of the tower

Solution. The horizontal projection AC is assumed unchanged by the inclination. Hence, this is the starting point, as it is common to both cases straight $\triangle ABC$ and inclined $\triangle AB'C$. At the beginning, we have a right triangle, hence the relation applies straightforward

$$AC = AB\cos(\alpha) = 2\cos(30) = 1.732km \tag{10}$$

However, the inclination changes the right triangle ($\angle ACB \equiv \gamma = 90$ deg) to a scalene triangle (with an angle change to $\angle ACB' \equiv \gamma' = 90 + 0.5 = 90.5$ deg), hence sine and cosine no longer apply directly. The extended versions given by Eq.(2) and Eq.(3) are applied in this case. The diagonal of the scalene triangle is given directly by the horizontal projection AC of the longest side AB´ giving

$$AB' = \frac{AC}{\frac{\sin(\alpha+\gamma')}{\sin(\gamma')}} = \frac{1.732}{\frac{\sin(30+90.5)}{\sin(90.5)}} = 2.010km \tag{11}$$

Therefore, the inclination of half a degree by the tower has stretched the main suspension cables by 10 meters.

4.2 Measuring Distances (E)

Problem. Imagine that civil engineers with theodolites devices (as in Figure 4a) are placed at either side of a river (at points A and B), and wish to measure their distance to a location on the bridge (at point C), which is inaccessible due to constructions (as in Figure 4b). Theodolites devices measure (among other things) vertical and horizontal angles between two visual reference points with great accuracy (Topcon Corporation, 2016). The difficulty, in this case, is that Point C is located on the bridge and directly over water, so it is not possible to measure the horizontal positions of point A and B to point C, and neither the height. However, the engineers can measure the distance between them, resulting in 200m. Engineer A rotates the theodolite from point B to C and measures a vertical angular distance of 38 degrees, while engineer B does the same from point A to C and measures 24 degrees. What are the distances of both engineers to point C on the bridge? What is the height from point C to the horizontal line connecting engineer A to B? And if the same line AB is inclined by ϵ = 10 degrees (α and β remaining the same), what is the height of point C to line AB?

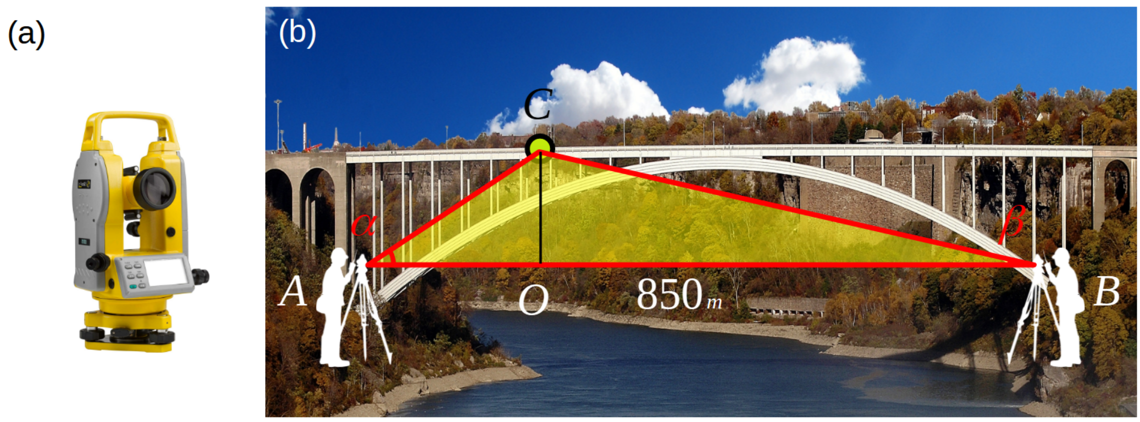

Figure 4. Finding distances from the shores to a point on an inaccessible bridge

Solution. The angle $\gamma = \angle ACB$ formed by the two theodolites at point C is 180-38-24=118 degrees. The distance of the first engineer A to point C on the bridge is given by the direct application of the extended cosine function as

$$AC = 200\cos^{*}(38, 118) = 200\left[\frac{\sin(38+118)}{\sin(118)}\right] = 92.1m \tag{12}$$

On the other hand, the distance of the second engineer B to point C on the bridge is given by direct application of the extended sine function as

$$BC = 200\sin^{*}(38, 118) = 200\left[\frac{\sin(38)}{\sin(118)}\right] = 139.5m \tag{13}$$

Knowing the distance and angle from A to C, it is simply a matter of applying conventional sine function to obtain the vertical projection in the right triangle $\triangle AOC$ as

$$CO = 92.1\sin(38) = 56.7m \tag{14}$$

If the line AB were to be inclined, making an angle ϵ = 10 degrees to the horizontal (here we assumed it is inclined to the left, as per Figure 5) — α = 38 degrees and β = 24 degrees remain the same — then the height of point C to line AB is (whilst remembering that the obtuse angle $\angle BO'C$ of triangle $\triangle BO'C$ in now 90 + ϵ = 100 degrees) given by the direct application of the extended sine function, as

$$CO' = BC \sin^*(\beta, 100) = 139.5\left[\frac{\sin(24)}{\sin(100)}\right] = 57.6m \tag{15}$$

Note that the added inclination (of 10 degrees) between the two theodolites A and B increased the vertical distance of point C to the line AB by almost 1 meter.

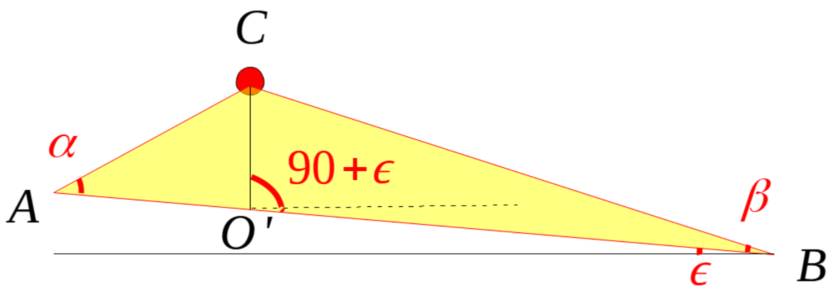

Figure 5. Finding distances from the shores to a point on an inaccessible bridge

5. Aerospace & Aeronautics

5.1 Turbine Velocity Triangles (E)

Problem. Velocity vector diagrams are tools used by aerospace and aeronautics engineers to design and understand the loading of a turbine stage on an aircraft engine (Figure 6a) (Haselbach & Taylor, 2013). It links the magnitude and direction of air velocity vectors (both absolute V_{ABS} and relative V_{REL} at the vane exit to rotor exit) with blade tangential speed U (Figure 6b). Imagine that the flow exiting a row of stator vanes has been measured to be 250 m/s at an absolute angle to the engine axis of $\theta = 70$ deg. The engineer selects a rotational speed for the rotor of 7,000 rpm. The mean blade diameter is 0.5m. What is the relative velocity V_{REL} seen by the rotor as the flow enters it (i.e., at the vane exit and rotor inlet plane)?

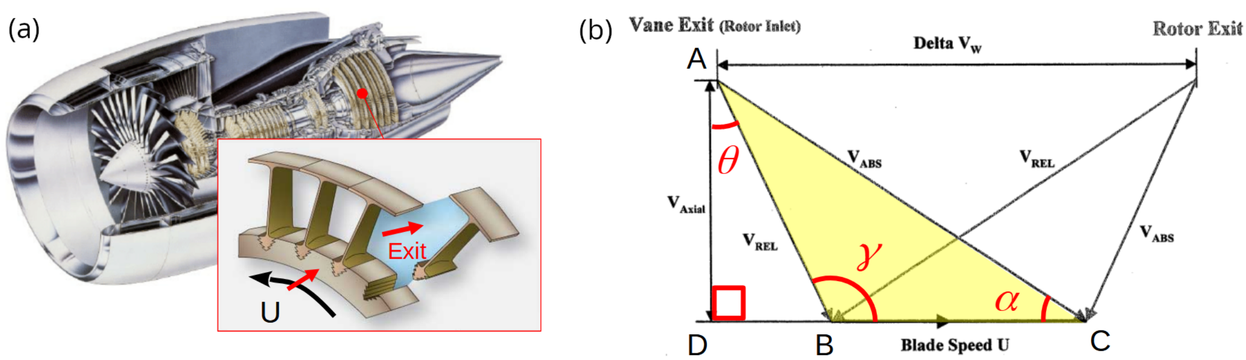

Figure 6. Velocity vector diagram for a turbine rotor blade in a turbofan engine

Solution. The analysis revolves around the scalene triangle $\triangle ABC$. At the stator exit plane, the air absolute velocity vector V_{ABS} makes an angle with the blade speed vector U of $\angle ACB \equiv \alpha = 180 - 90 - 70 = 20$ deg. The rotational speed 7,000 rpm is converted to mean blade tangential velocity U as

$$U = \frac{7000}{60} * 2\pi D = 157.1m/s \tag{16}$$

Finding the angle $\gamma \equiv \angle ABC$

$$V_{ABS} \cos^*(\alpha, \gamma) = V_{ABS}\left[\cos(\alpha) + \frac{\cos(\gamma)}{\sin(\gamma)} \sin(\alpha)\right] \tag{17}$$

which, by replacing the values above, results in

$$U = 157.1 = 250\left[\cos(20) + \frac{1}{\tan\gamma}\sin(20)\right] \tag{18}$$

That re-arranged gives

$$\tan(\gamma) = \frac{\sin(20)}{\frac{157.1}{250} - \cos(20)} = -1.098 \tag{19}$$

Note that, computing the arctangent of angle γ gives -47.7 degrees. Since we know that the angle γ needs to be obtuse, we add 180 degrees to give $\gamma = 132.3$ degrees (the tangent is the same for both angles). To find the relative velocity V_{REL}, one simply applies the $\sin^*(\alpha, \gamma)$ expression (i.e., project side AC onto AB), which gives

$$V_{REL} = V_{ABS}\sin^*(20, 132.3) = 250\left[\frac{\sin(20)}{\sin(132.3)}\right] = 115.6m/s \tag{20}$$

If the absolute angle of V_{ABS} to the engine axis θ is in fact 2 degrees more than anticipated, what is the new relative velocity V_{REL} (use the angle difference identity rule)?

The new angle is $\theta = 70 + 2 = 72$ deg, which based on the internal angle sum of the triangle $\triangle ADC$, gives a angle $\alpha = 180 - 90 - 72 = 20 - 2 = 18$ deg. For the same mean blade tangential velocity U, the obtuse angle of triangle $\triangle ABC$ becomes

$$\tan(\gamma) = \frac{\sin(20-2)}{\frac{157.1}{250} - \cos(20-2)} = 0.7358 \tag{21}$$

As before the resulting obtuse angle is $\gamma = 136.2$ deg. To find the relative velocity V_{REL}, one applies the angle difference identity rule for $\sin^*(A - B, \gamma)$ [given by Eq.(8)]

$$V_{REL} = V_{ABS}\sin^*(20-2, 136.2) = 157.1\left[\sin^*(20-2, 136.2)\right] \tag{22}$$

which expands to

$$\sin^*(20-2, 136.2) = \sin^*(20, 136.2)\cos^*(2, 136.2) - \cos^*(2 - 180 + 2\times 136.2, 180 - 136.2)\sin^*(2, 136.2) \tag{23}$$

By applying the extended sine and cosine functions given by Eq.(2) and Eq.(3), the end result is $V_{REL} = 104.4m/s$. The two degree increase of the inlet absolute angle represents a reduction of the perceived relative velocity for the rotor of approximately 11m/s.

5.2 Aircraft Flight Path (E)

Problem. Two engineers placed theodolites (height 1.7m) at a distance of 400m apart over a runway to record the flight path of aircraft taking off. One aircraft departs and climbs directly over them. As it crosses the sky, the engineers measure at either side the vertical angle for different synchronized times. The usage of electro-optical system to track the position of aircraft is common in the world of aviation (Wuhan Huazhiyang Technology Corporation, 2020). The result are a succession of scalene triangles, as illustrated in Figure 7 (with the recorded angles presented on the right). What is the distance of the aircraft to each of the points A and B in the ground? Subsequently, what is the height of the aircraft at the different points in time (with respect to the theodolites measuring position)?

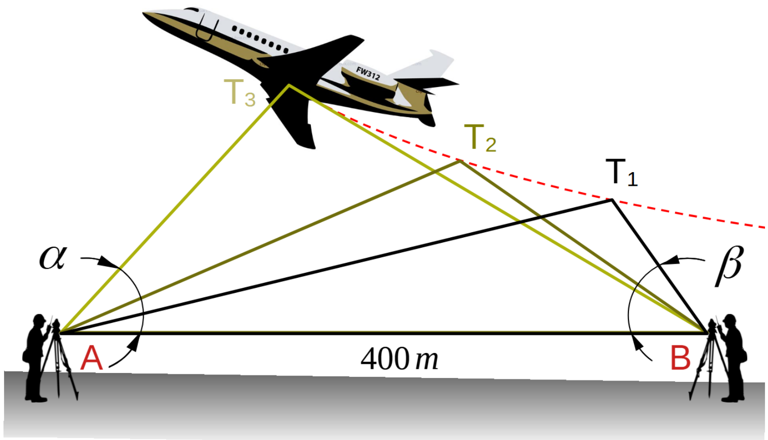

T	α	β
T_1	19°	45°
T_2	32°	39°
T_3	73°	28°

Figure 7. Measurement of aircraft flight trajectory during climb

Solution. Drawing lines from the three elements — engineers A, B and the aircraft — created a series of scalene triangles that change based on the time of flight of the aircraft. Using the three ground angles for both α and β measured with the theodolites, the third internal angle γ of each scalene triangle was computed to be 116 degrees for T1, 109 degrees for T2 and 79 degrees for T3. The solution for each aircraft position with associated time is computed directly from the extended formula. For time T1, the distance from engineer A to the aircraft is

$$AT_1 = 400 \cos^*(19, 116) = 400\left[\frac{\sin(19+116)}{\sin(116)}\right] = 191.3m \tag{24}$$

and the distance to engineer B is

$$BT_1 = 400 \sin^*(19, 116) = 400\left[\frac{\sin(19)}{\sin(116)}\right] = 144.9m \tag{25}$$

and the aircraft is at a vertical distance of

$$h_1 = 314.7.9 \sin(19) = 102.5m \tag{26}$$

For time T2, the aircraft is at a distance from engineer A of

$$AT_2 = 400 \cos^*(32, 109) = 400\left[\frac{\sin(32+109)}{\sin(109)}\right] = 224.2m \tag{27}$$

and a distance from engineer B of

$$BT_2 = 400 \sin^*(32, 109) = 400\left[\frac{\sin(32)}{\sin(109)}\right] = 266.2m \tag{28}$$

while the aircraft is at a vertical distance of

$$h_2 = 224.2 \sin(32) = 141.1m \tag{29}$$

For time T3, the distance from engineer A to the aircraft is

$$AT_3 = 400 \cos^*(73, 79) = 400\left[\frac{\sin(73+79)}{\sin(79)}\right] = 191.3m \tag{30}$$

and the distance from engineer B is

$$BT_3 = 400 \sin^*(73, 79) = 400\Big[\frac{\sin(73)}{\sin(79)}\Big] = 389.7m \tag{31}$$

and the aircraft is at a height of

$$h_3 = 191.3 \sin(73) = 182.9m \tag{32}$$

Now, if the aircraft projects a shadow on the ground at an angle of 20 degrees to the vertical, what is the distance from engineer A to the projection at point O (Figure 8)? If the reading of the theodolite at A increases by an angle of $d\alpha = 10$ degrees as the aircraft climbs (here, we assume that the aircraft rotation or flight path is such that its relative distance to point A remains the same, i.e. $AT_2 = AT_2'$), what is the new distance from engineer at point A to the new shadow at point O' (use the angle sum identity rule)?

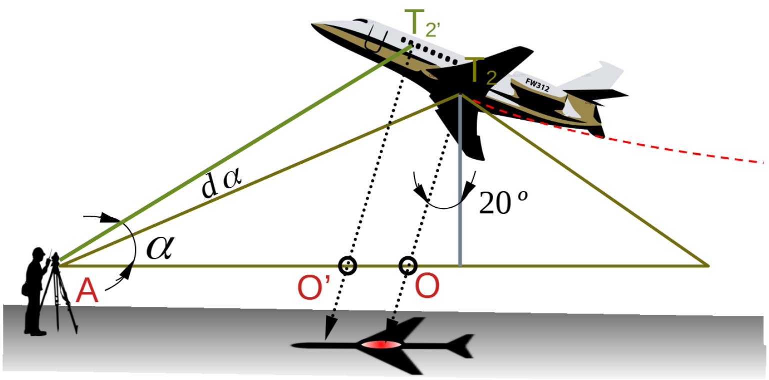

T	α	β
T_1	19°	45°
T_2	32°	39°
T_3	73°	28°

Figure 8. Measurement of the shadow location of the aircraft

The angle from the horizontal to the projected direction of the shadow is $\angle AOT_2 \equiv \gamma = 90 + 20 = 110$ deg. For position T2, the extended cosine function gives directly the answer for the distance from point A to the projected shadow on the ground to be

$$AO = AT_2 \cos^*(32, 110) = 224.2\left[\frac{\sin(32 + 110)}{\sin(110)}\right] = 146.9m \tag{33}$$

The fact that the relative distance of the aircraft does not change with respect to point A means that, as the aircraft rotates in its climb, the distance $AT_2 = AT_2' = 224.2m$ (in Figure 8) remains fixed. The extended angle sum identity rule [given by Eq.(7)] is used here to determine the new distance from engineer at point A to the new shadow at point O'. With the rotation, the original angle $A \equiv \alpha_2 = 32$ deg becomes $A + B = \alpha_2 + d\alpha = 32 + 10 = 42$ deg. The new horizontal projection of the shadow becomes thus

$$AO' = AT_2' \cos^*(A + B, \gamma) \tag{34}$$

The projected direction of the shadow is still $\angle AOT_2' \equiv \gamma = 110$ deg (as the Sun's rays are assumed parallel when they arrive at Earth). Expanding the above using Eq.(7) gives

$$AO' = 224.2\Big[\cos^*(32, 110)\cos^*(10, 110) - \sin^*(32, 180 - 110)\sin^*(10, 110)\Big] = \tag{35}$$

$$= 224.2\left[\frac{\sin(32 + 110)}{\sin(110)}\frac{\sin(10 + 110)}{\sin(110)} - \frac{\sin(32)}{\sin(180 - 110)}\frac{\sin(10)}{\sin(110)}\right] = 112m$$

That is, the shadow moved from 146.9m to a distance from engineer A of 112m meters, a total distance covered of 34.9m. The advantage of Eq.(7) becomes evident when considering $d\alpha$ as a variable (possibly part of a larger equation). Imagine that you would like to know where the shadow was (for both positions) for a different time of the day (say when the Sun was at an angle to the vertical of 10 deg, instead of 20 deg). Then, it is only required to re-apply the above equations, updating with the new Sun incidence angle of $\gamma = 90 + 10 = 100$ degrees (here it is assumed that the aircraft flight path would remain the same).

5.3 Satellite Constellation Orbit (E)

Problem. Imagine three GPS satellites trailing each other on the same orbit. It is assumed that they operate best at a given (normalized) relative position to each other (as shown in Figure 9). It is worth noting that this is an abstraction, as in reality such a constellation of properly geometrically-spaced GPS satellites orbiting the Earth typically has 24 satellites disposed in a 3D configuration (Moorefield Jr., 2020) — so this is a very simplified example. Here, each satellite has an optical sensor onboard that measures the satellite´s angle between the others two. What angles do the sensors of all three need to measure to guarantee that they are flying at the target (normalized) orbital distance to each other?

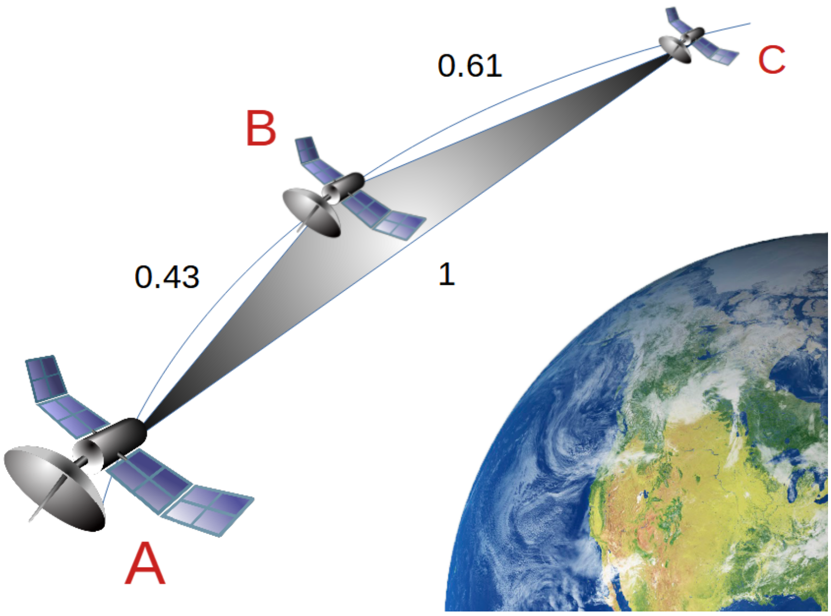

Figure 9. Satellite constellation flying in a specific target formatio

Solution. Since the sum of the internal angles of a triangle is 180 degrees, all is required is to know two of them. This implies the need of two equations to solve two variables. The first equation results from the cosine projection of the longest side of the scalene triangle as

$$BC = 0.61 = \sin^*(\alpha, \gamma) = \frac{\sin(\alpha)}{\sin(\gamma)} \tag{36}$$

which re-arranged gives

$$\sin(\gamma) = \frac{\sin(\alpha)}{0.61} \tag{37}$$

Similarly, the cosine projection of the longest side of the scalene triangles gives

$$AB = 0.43 = \cos^*(\alpha, \gamma) = \cos(\alpha) + \frac{\sin(\alpha)}{\sin(\gamma)}\cos(\gamma) \tag{38}$$

By replacing the above result in

$$0.43 = \cos(\alpha) + \frac{\sin(\alpha)}{\frac{\sin(\alpha)}{0.61}}\cos(\gamma) \tag{39}$$

that simplifies to

$$\cos(\gamma) = \frac{0.43 - \cos(\alpha)}{0.61} \tag{40}$$

Replacing Eq.(37) and Eq.(40) into the identity rule $sin^2(\gamma) + cos^2(\gamma) = 1$ results in

$$\left(\frac{\sin(\alpha)}{0.61}\right)^2 + \left(\frac{0.43}{0.61} - \frac{cos(\alpha)}{0.61}\right)^2 = 1 \tag{41}$$

Expanding results in

$$\left(\frac{\sin(\alpha)}{0.61}\right)^2 + \left(\frac{0.43}{0.61}\right)^2 - 2\left(\frac{0.43}{0.61}\right)\left(\frac{\cos(\alpha)}{0.61}\right) + \left(\frac{\cos(\alpha)}{0.61}\right)^2 = 1 \tag{42}$$

Placing the denominator to the right side simplifies this to

$$\sin^2(\alpha) + 0.43^2 - 2(0.43)\cos(\alpha) + cos^2(\alpha) = 0.61^2 \tag{43}$$

which reduces further to

$$1 + 0.43^2 - 2(0.43)cos(\alpha) = 0.61^2 \tag{44}$$

resulting in an expression for $cos(\alpha)$ as

$$cos(\alpha) = \frac{1 + 0.43^2 - 0.61^2}{2(0.43)} \tag{45}$$

Note that, computing the arcsine of angle γ gives 32.39 degrees which is in the first quadrant. Since we know that the angle γ needs to be obtuse, we are interested in the value in the second quadrant of 147.61 degrees which has the same value of sine. The third angle β then becomes

$$\beta = 180 - \alpha - \gamma = 180 - 19.07 - 147.61 = 13.32 \tag{46}$$

Therefore, in order for the satellites to fly at the target normalized distance to each other (as per values shown in Figure 9), the angular sensor in satellite A needs to measure 19.07 degrees (between satellite B and C), the one in satellite B needs to measure 147.61 degrees (between satellite A and C) and satellite C needs to read 13.32 degrees (between satellite A and B).

6. Telecommunications

6.1 Antenna Array Beamforming and Steering (P)

Possibility. Imagine an antenna array composed of sensing elements uniformly spaced in a line. *Beamforming* is a process by which an interference pattern between the radiated or received signals of all the antenna elements allows the array to acquire directivity in reception/emission, by forming a high gain lobe (in which it is most sensitive to transmissions) located at the center of the array, and perpendicular to the array's axis (Liu & Weiss, 2010). This process involves the use of sine functions and trigonometry, and hence we will expand further into its workings. When two antenna elements are spaced by distance d (Figure 10a), and angled by α to the incoming transmitted wave front (each successive antenna elements will record the same wave with a delay), where this lag is trigonometrically governed by a right-angled triangle inherently governed by the Pythagoras theorem. This forms the basis for the processing required to calculate the array's gain sensitivity to direction or beamforming. If X(t) is the signal received by the antenna element 0 (Figure 10a), then antenna element 1 receives the same signal (as element 0) with a time delay τ, expressed mathematically as

$$X_1(t) \cong X(t - \tau) \qquad \text{with} \qquad \tau = \frac{d}{c}\sin(\alpha) \tag{47}$$

The gain of an array is typically computed from the summation of all signals, and is used to construct the array radiation pattern, quantifying its directivity. For these two particular elements, the time delay τ occurs due to the waves angle of arrival α — i.e. the extra distance BC that the EM waves need to cover due to the inclination α of the antenna array —

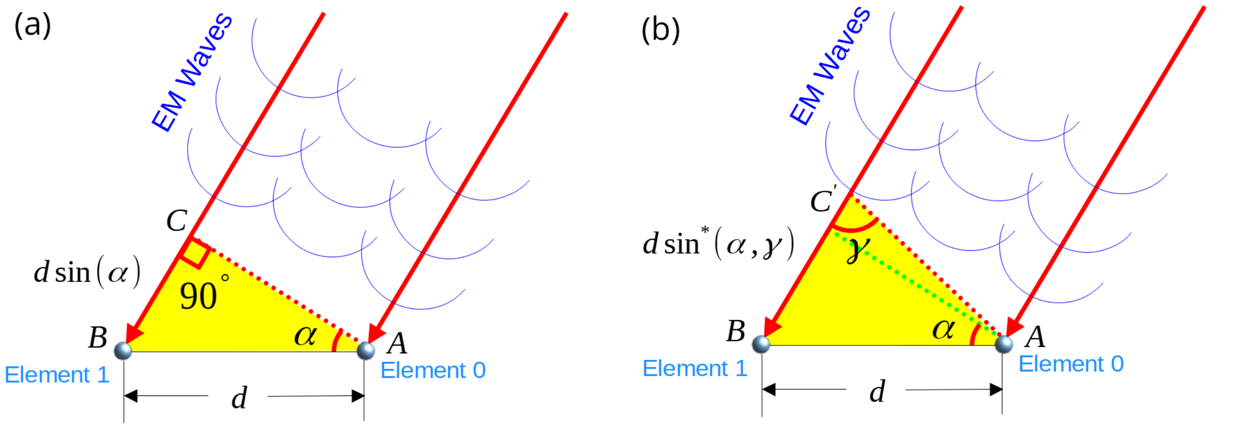

Figure 10. Time delay in reception of EM wave in a linear antenna array governed by (a) right and (b) scalene triangles

thus forming with the distance $d = BA$ in between elements a right triangle $\triangle ABC$, where c is the speed of light in the medium air (close to that in vacuum), and d is the distance between successive elements. *Beam steering* is a process that provides the ability to change the direction of an incoming or outgoing beam on a uniform linear antenna array, and it is achieved by introducing an arbitrary time delay Δt between each subsequent pair of antenna elements. This alters the signal received/emitted by element 1 into

$$X_1(t) \cong X(t - \tau - \Delta t) \qquad \text{with} \qquad \tau' = \frac{\delta}{c}\sin^*(\alpha, \gamma) \tag{48}$$

In reality, this time delay Δt can be interpreted as a distortion in the trigonometric relation between the distances composing the right triangle $\triangle ABC$. Geometrically, the time delay Δt is translated into an added distance, transforming BC (Figure 10a) into BC' (Figure 10b). This consequentially transforms the right triangle $\triangle ABC$ (Figure 10a) into the scalene triangle $\triangle ABC'$ (Figure 10b). The new time delay τ' in Eq.(48) indicates that $\tau'(\alpha, \gamma)$ accounts for the two delay components: (1) delay between successive elements due to array inclination and element spacing — the original τ [this is governed by angle α and forms the right triangle $\triangle ABC$], and (2) the fictitious delay introduced mathematically resulting in the artificial elongation/reduction of the wave travel distance (that compounds with the array elements) [the alteration of angle γ morphs the right triangle into a scalene triangle; the difference of the base of the two defines this delay]. Thus, the extended sine function enables the signal mathematical expression to change to

$$X_1(t) \cong X(t - \tau'(\alpha, \gamma)) \qquad \text{with} \qquad \tau'(\alpha, \gamma) = \frac{\delta}{c}\left[\frac{\sin(\alpha)}{\sin(\gamma)}\right] \tag{49}$$

where $\sin(\alpha)$ governs the directivity of the antenna array [via the control of angle α], and $\sin(\gamma)$ governs the direction of the emitted/received signal [via the angle γ]. Hence, both the influence of τ and Δt can be modeled within one expression, and controlled via two angles α and γ. Since the fundamental operating principle of beamforming is the same between 2D and 3D, by legacy the application of the proposed modification (of the mathematical modelling using the extended sine function) could be extended to three dimensional beamforming.

6.2 Enhancing Data Aerial Transmission (P)

Possibility. Binary digital modulation techniques (used in modern wireless data transmission) are simple in concept, but are not efficient in terms of their spectral density. Augmentation of spectral efficiency (i.e., boost transmission bit rate without affecting bandwidth requirements) is commonly achieved via the adoption of quaternary signaling schemes, like quadrature phase-shift keying (QPSK) (Grami, 2016). In QPSK, the number of bits that are combined are 2 so this makes four phase shifts posssible. Quaternary signaling schemes embed information in carrier phase modifications, while at the same time keeping the carrier amplitude and frequency the same. Digital signals Q and I are used to modulate a carrier wave by altering its phase in four possible ways (i.e., 45, 135, 225 and 315 degrees), each representing a symbol (Figure 11a). The in-phase signal I is along the x-axis in Figure 11a, and is represented in magenta in Figure 11b. The quadrature signal Q is along the y-axis in Figure 15a, and is represented in blue in Figure 11b. In an orthogonal system of axis, the x-axis is at 90 degrees to the y-axis, which means that the in-phase signal I is phase shifted by 90 degrees from the quadrature signal Q. The novelty introduced by the extended sine and cosine functions is in the ability to change the angle between the system's axis (other than $\gamma = 90$ deg), providing the potential to increase the keys available by having two (or more) interchangeable system of axis in operation. The digital QPSK modulated signal is given by the equation

$$S(t) = A_C \Big\{ \Big[\sin(\phi)\sin(\alpha) \Big]_Q + \Big[\cos(\phi)\cos(\alpha) \Big]_I \Big\} \tag{50}$$

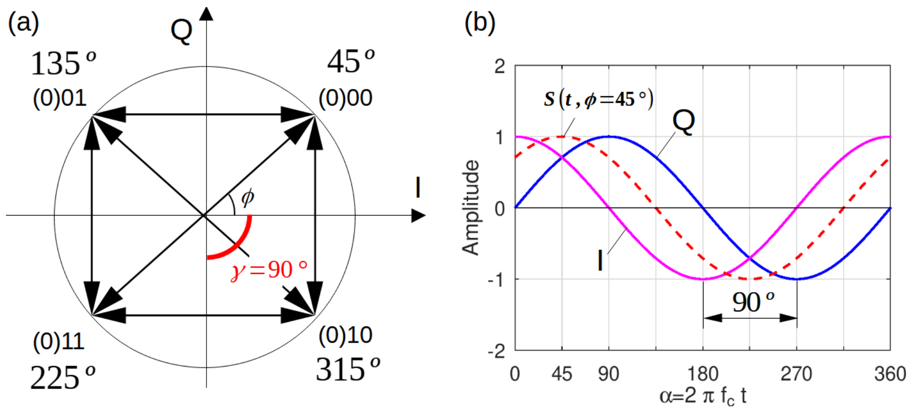

Figure 11. Quadrature Phase Shift Keying Modulation [QPSK]: (a) symbols possible and (b) phasing of carrier wave

where angle ϕ controls the normalized amplitude of the carrier signals Q and I — such that when they add up, the carrier is perceived to undergo a phase shift (i.e. ϕ =45, 135, 225 or 315 deg) — and angle $\alpha = 2\pi f_c t$ governs the oscillation of the carrier and modulated waves with time. The amplitude of the signal is given as $A_c = \sqrt{2E/T}$, where $E = P \times T$ (i.e., power times time interval) is the energy content in a bit duration. In other words, changing ϕ offsets in Figure 11b the dashed line horizontally back and forth. The coefficients that enable the carrier to shift by the above desired phases are given in Table 1.

Table 1. Coefficients of modulated signal for $\gamma = 90$ deg

ϕ (deg) - binary	$m_Q(t) = \sin(\phi)$	$m_I(t) = \cos(\phi)$
45 - (0)00	$\sqrt{2}/2$	$\sqrt{2}/2$
135 - (0)01	$\sqrt{2}/2$	$-\sqrt{2}/2$
225 - (0)10	$-\sqrt{2}/2$	$-\sqrt{2}/2$
315 - (0)11	$\sqrt{2}/2$	$-\sqrt{2}/2$

Until now, the phase distance between the carrier wave Q and I was fixed to 90 degrees, as sine and cosines are governed by the dynamics of a right-angled triangle. With the extended sine and cosines functions, this phase distance can be modified to an arbitrary value given by the angle γ. Since the system axes are now no longer static (frozen in orthogonal mode), this approach is hereby termed the Dynamic-Axis Quadrature Phase Shift Keying Modulation or DA-QPSK Modulation. Replacing the sine and cosine by their extended functions in Eq.(2) and Eq.(3), allows the x-axis to be at virtually any angle γ to the y-axis, which means that the in-phase signal I is phase shifted by angle γ from the quadrature signal Q. Digital signals Q and I are used to modulate a carrier wave by altering its phase in four possible ways (i.e., 45, 135, 225 and 315 degrees), each representing a symbol (Figure 11a). Figure 12a shows that by altering the angle between the two axes (in this case, to $\gamma = 120$ degrees) allows the creation of additional four phases (i.e., 30, 120, 210 and 300 degrees) or symbols different from Figure 11a. Note that these phase angles are associated with a system of axis (i.e., $\gamma = 120$ degrees) different from the orthogonal (i.e., $\gamma = 90$ degrees), and thus a 120 degrees has different meaning in either system of axes. For the case where $\gamma = 120$ degrees, the in-phase signal I has a 120 degree phase shift from the quadrature signal Q (Figure 12b). The amplitude modulations of the quadrature signal Q and in-phase signal I produce the phase-shifting of the wave produced by their sum (dashed red in Figure 12b for $\phi = 30$ deg implying symbol 100) — of the same frequency and amplitude as the carriers — is given as follows

$$S(t, \gamma, \phi) = \Big[sin^*(\phi, \gamma)\sin^*(\alpha, \gamma) \Big]_Q + \Big[cos^*(\phi, \gamma)\cos^*(\alpha, \gamma) \Big]_I \tag{51}$$

where ϕ is the phase shift of the modulated signal with respect to Q, and controls via the extended sine and cosine coefficients the amplitudes of both Q and I such that the their sum is always constant. Note that the generalized Eq.(51)

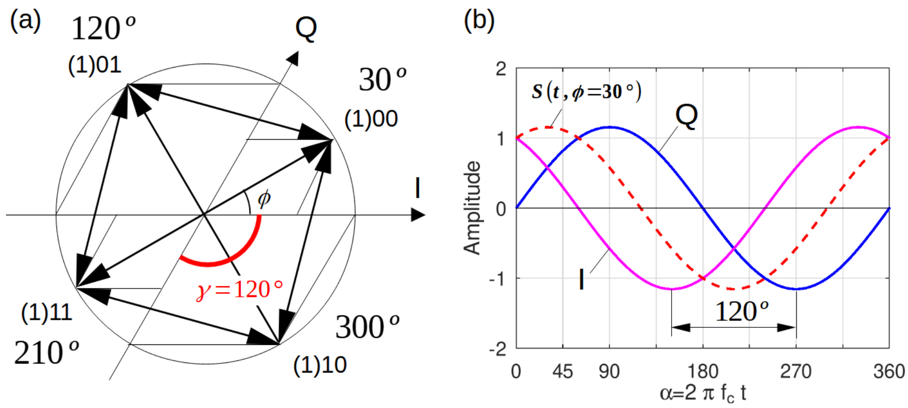

Figure 12. Dynamic-Axis Quadrature Phase Shift Keying Modulation [DA-QPSK]: (a) symbols and (b) phases of carrier

encompasses the particular cases of Figure 11 where γ = 90 deg and Figure 12 where γ = 120 deg. In both cases it produces a wave, same as the carrier, except it has a phase offset. Equation (51) can be written in a more compact manner as

$$S(t,\gamma,\phi) = \left[m_Q^*(t)\sin^*(\alpha,\gamma)\right]_Q + \left[m_I^*(t)\cos^*(\alpha,\gamma)\right]_I \tag{52}$$

where the extended $m_Q^*(t)$ and $m_I^*(t)$ functions are determined by expanding using Eq.(2) and Eq.(3) as

$$m_Q^*(t) = sin^*(\phi,\gamma) = \frac{\sin(\phi)}{\sin(\gamma)} \quad ; \quad m_I^*(t) = cos^*(\phi,\gamma) = \frac{\sin(\phi+\gamma)}{\sin(\gamma)} \tag{53}$$

For the particular case of an orthogonal axis system (γ = 90 deg), the above functions reduce back to the original versions $m_Q^*(t,90) = \sin(\phi)$ and $m_I^*(t,90) = \cos(\phi)$. As an example of its application, let us conceive a change in the angle formed between the y-axis for Q and x-axis for I to the particular case of γ = 120 degrees. In such a case, the extended function $m_Q^*(t)$ becomes

$$m_Q^*(t) = \sin^*(\phi,120) = \frac{\sin(\phi)}{\sin(120)} = \frac{2}{\sqrt{3}}\sin(\phi) \tag{54}$$

and the extended function $m_I^*(t)$ becomes

$$m_I^*(t) = \cos^*(\phi,120) = \frac{\sin(\phi+120)}{\sin(120)} = \frac{2}{\sqrt{3}}\left\{\sin(\phi)\left(-\frac{1}{2}\right) + \cos(\phi)\frac{\sqrt{3}}{2}\right\} \tag{55}$$

which re-arranged further simplifies to

$$m_I^*(t) = -\frac{1}{\sqrt{3}}\sin(\phi) + \cos(\phi) \tag{56}$$

For the particular case of γ = 120 deg, the signal expression in Eq.(51) transforms to

$$S(t,120,\phi) = \left[\left\{\frac{2}{\sqrt{3}}\sin(\phi)\right\}\sin^*(\alpha,120)\right]_Q + \left[\left\{-\frac{1}{\sqrt{3}}\sin(\phi)+\cos(\phi)\right\}\cos^*(\alpha,120)\right]_I \tag{57}$$

Consider the case of the symbol 100 (in the first quadrant, where ϕ = 30 deg). Then the function $m_Q^*(t)$ [given by Eq.(54)] becomes the fractional number

$$m_Q^*(t) = \sin^*(30,120) = \frac{2}{\sqrt{3}}\sin(30) = \frac{2}{\sqrt{3}}\left(\frac{1}{2}\right) = \frac{\sqrt{3}}{3} \tag{58}$$

Similarly, the function $m_I^*(t)$ [given by Eq.(56)] becomes also a fractional number

$$m_I^*(t) = -\frac{1}{\sqrt{3}}\sin(30) + \cos(30) = -\frac{1}{\sqrt{3}}\left(\frac{1}{2}\right) + \frac{\sqrt{3}}{2} = \frac{\sqrt{3}}{3} \tag{59}$$

Thus, the coefficients that enable the carrier to shift by the above desired phases (i.e., 30, 120, 210 and 300 degrees) can be computed using the same approach as above, resulting in Table 2.

Table 2. Coefficients of modulated signal for $\gamma = 120$ deg

ϕ (deg) - binary	$m_Q^*(t)$	$m_I^*(t)$
30 - (1)00	$\sqrt{3}/3$	$\sqrt{3}/3$
120 - (1)01	1	-1
210 - (1)10	$-\sqrt{3}/3$	$-\sqrt{3}/3$
300 - (1)11	-1	1

Figure 13 shows an example of the conceptual block diagram of the transmitter that could produce the Dynamic-Axis QPSK modulation. The new key difference between DA-QPSK and classical QPSK modulation is highlighted with a red box, representing the ability to alter the phase between the Q and I carrier waves beyond the customary 90 degrees — a choice that is controlled by the binary status of the first of the 3 Bits via an additional switch. Hence, in DA-QPSK, the number of bits that are combined are 3 so this makes for eight phase shifts possible (an improvement from QPSK, where only four are available).

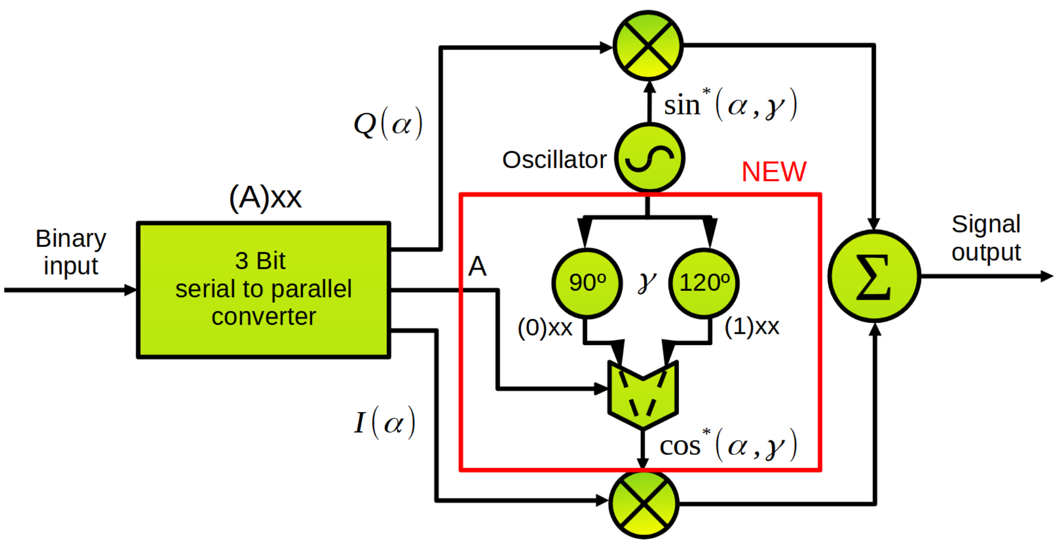

Figure 13. Transmitter block diagram for the Dynamic-Axis QPSK modulation

The reception and interpretation of the signal implies, for each phase change determine what is the magnitude. If it is an angle multiple of 90/2=45 degrees, then the first digit is 0. Likewise, if it is a multiple of 120/2=60 degrees, then the first digit is 1. So, the first digit is determined by the resulting factorization of the phase. Second, the other two digits are determine by the magnitude of the phase, and is located in the axes plus circle diagram in the same manner as for QPSK modulation. The only difference here, is that if the first bit is 1, then the 120 degree system of axis is used, and the location in the diagram will change [according to Eq.(54)].

7. Conclusion

Problem solving in physics is directly dependent on the level of sofistication of available mathematical tools. The Pythagoras theorem, and its dependent sine and cosine functions, have been mathematical pilars that have enabled the solution of a variety of physical problems, ranging from simplistic mass-spring oscilatory system to quantum resonators. Generalization of trigonometry involving the replacement of the Pythagoras theorem (the exception) by the Law of Cosines (the rule), results in a new set of extended or gamma sine and cosine functions, which have already been proven and published. These new mathematical formulae open doors for a fresh approach to tackle problems in physics, and enable a depeer insight into the trigonometric relations within physical problems for a variety of fields:

- **Civil Engineering**: The impact of a slight rotation of a tower in a *suspension bridge* on the stretching of its cables is assessed simply by using one formula. *Measuring distances* to an inacessible bridge over a river using two engineers with theodolites is accomplished by carefull application of the new extended or gamma trigonometric functions.
- **Aerospace & Aeronautics**: *Turbine velocity triangles* are a fundamental trigonometric tool often adopted when designing turbine stages (stator plus rotor), as they provide both absolute (with respect to the stator) and relative (with respect to the rotor) air speed, for any given turbine rotational speed. Impact of slight variations of inlet angle on speed is also computed to get an indication on how one affects the other, particularly useful since rotor turbine inlet conditions in reality always vary with respect to target design conditions. Moreover, a study is conducted on a simplified *GPS satellite constelation*, where the extended or gamma trigonometry functions are used in conjunction with optical sensors installed in each satellite, to determine if all satellites are at the hypothetical predefined optimum orbital position. Finally, the flight path of an aircraft during take-off can be tracked via two engineers with theodolites, and carefull application of the gamma trigonometric functions, to determine how high it is from the ground at each given point in time.
- **Telecommunications**: A couple of improvement possibilities are presented: one with respect to *antenna array beamforming and steering*, namely in the mathematical construct used to describe the signal received based on the antenna dimensions and angle of incoming waves (i.e., the linear dimensions are replaced by angles that control the beamforming and steering effects); the second with respect to enhancing *data aerial transmission* (e.g., quadrature phase-shift keying or QPSK), namely by introducing a new means to control the carrier wave such that a series of new four phase shifts are possible (other than the original), allowing for the transmission to increase to three bits per signal (an increase from two bits per signal in the classical QPSK). This effetively increases the transmission bit rate without affecting bandwidth requirements. The newly derived modulation technique is herein termed the dynamic-carrier quadrature phase-shift keying or DC-QPSK, due to the added flexibility in the dynamics of the carrier wave. The geometry and mathematics of wave propagation — here presented in the field of telecommunications (i.e., electromagnetic wave propagation in space) — is shared to some degree by acoustics (i.e., pressure wave propagation in air), and thus similar problems in acoustics could be addressed using the new gamma trigonometric functions (e.g., beamforming techniques applied in a linear array of microphones to track noise sources).

Applications in many other subjects involving trigonometry are also possible, like for instance in mechanical oscilatory systems, electrical motors and generators (looking at the analysis of phase diagrams), antenna arrays (how mobile phone signals behaves as it rotates around antenna array), mechanical systems such as cranes and complex machines (for computation of stress distributions and deflections, for example), relativistic theory and the time dialation effect, electronics such as the new energy-coupled RLC circuit (looking at voltage and current behaviour under dynamic oscilatory conditions for when capacitance and inductance ffects are coupled — to be further discussed in a future publication), etc. The aim of this article is to given an impression on how these more flexible and advanced gamma trigonometric functions (because the gamma sine and cosine functions incorporate the variation of two angles α and γ in a scalene triangle, versus just the one angle α in a right-triangle for the classical sine and cosine) can be applied in practice, and by similarity be employed, be employed in other scientific fields and physical contexts. The present limitation of this research derives from the fact that it is so new, and all the ramifications to various different scientific fields are yet to be explored. Essentially, the extended (or gamma) sine and cosine functions replace the role of the traditional sine and consine versions in all the fields were these trigonometric functions are employed. They open doors to the expansion of the above pool of exercises to a vast number of other topics, like for example biology, architecture, informatics, electronics, not to mention the implication on hyperbolic trigonometry and modern geometry. It is therefore, both wanted and expected, that follow-on articles apply these mathematical tools to other avenues of physical and mathematical research, with the findings ideally being published in this journal, and preferably in a fashion complementary to this article.

References

Australian Curriculum, Assessment and Reporting Authority. (n.d.). Australian curriculum: Mathematics F–10. Retrieved from http://www.australiancurriculum.edu.au

Canadian Ministry of Education. (2020). The Ontario Curriculum, Grades 1–8: Mathematics. Retrieved from https://www.dcp.edu.gov.on.ca/en/curriculum/elementary-mathematics

Curtis, H. D. (2010). *Orbital Mechanics for Engineering Students* (2nd ed.). Butterworth-Heinemann. https://doi.org/10.1016/C2009-0-19374-1

Feng, G. T. (2013). Introduction to Geogebra – Version 4.4. Retrieved from https://www.academia.edu/3489 0249/Introduction_to_Introduction_to_GeoGebra

Grami, A. (2016). *Introduction to Digital Communications.* Academic Press. https://doi.org/10.1016/C2012-0-06171-6

Haselbach, F., & Taylor, M. (2013). *Axial Flow High Pressure Turbine Aerodynamic Design.* Lecture Series—Von Karman Institute for Fluid Dynamics. Chap. 7.

Howard Mark, H., & Workman Jr. J. (2018). *Chemometrics in Spectroscopy* (2nd ed.). Academic Press. https://doi.org/10.1016/C2015-0-04023-0

Liu, W., & Weiss, S. (2010). *Wideband Beamforming - Concepts and Techniques.* John Wiley & Sons Inc. New York.

Maor, E. (2007). *The Pythagorean Theorem: A 4,000 Year History.* Princeton University Press. Retrieved from https://www.jstor.org/stable/j.ctvh9w0ks

Moorefield Jr., F. D. (2020). GPS Standard Positioning Service (SPS) Performance Standard. Office of the Department of Defense. U.S. Government. Retrieved from https://www.gps.gov/technical/ps/2020-SPS-performance-standard.pdf

Parisher, R. A., & Rhea, R. A. (2012). *Pipe Drafting and Design* (3rd ed.). Gulf Professional Publishing. https://doi.org/10.1016/C2011-0-06090-8

Pickover, C. A. (2012). *The Math Book: From Pythagoras to the 57th Dimension, 250 Milestones in the History of Mathematics.* Sterling Milestones.

Pipinato, A. (2021). *Innovative Bridge Design Handbook: Construction, Rehabilitation, and Maintenance* (2nd ed.). Elsevier. https://doi.org/10.1016/C2019-0-05398-8

Rawlins, J. C. (2000). *Basic AC Circuits* (2nd ed.). Newnes Publishing. https://doi.org/10.1016/B978-0-7506-7173-6.X5000-7

Reys, B. J., Dingman, S., Nevels, N., & Teuscher, D. (2007). High School Mathematics: State-Level Curriculum Standards and Graduation Requirements. Center for the Study of Mathematics Curriculum. Retrieved from https://files.eric.ed.gov/fulltext/ED535222.pdf

Teia, L. (2021a). Extended Pythagoras Theorem using Triangles, and its Applications to Engineering. *The Journal of Open Engineering*. https://doi.org/10.21428/9d720e7a.7b128995

Teia, L. (2021b). Extended Pythagoras Theorem Using Hexagons. *Journal of Mathematics Research, 13*(6), 46-51. https://doi.org/10.5539/jmr.v13n6p46

Teia, L. (2022c). Extended Sine and Cosine Functions for Scalene Triangles. *Journal of Mathematics Research, 14*(5), 36-45. https://doi.org/10.5539/jmr.v14n5p36

Teia, L. (2022d). Extended Angle Sum and Difference Identity Rules for Scalene Triangles. *Journal of Mathematics Research, 14*(5), 21-35. https://doi.org/10.5539/jmr.v14n5p21

Teia, L. (2023). Gamma Derivatives for the Upgraded Mass-Spring Oscillatory System. *Journal of Mathematics Research, 15*(1), 57-74. https://doi.org/10.5539/jmr.v15n1p57

Timoshenko, S. P., Young, D. H., & Weaver, W. (1974). *Vibration Problems in Engineering* (4th ed.). John Wiley & Sons Inc., New York. Retrieved from https://archive.org/details/vibrationproblem031611mbp/mode/2up

Topcon Corporation. (2016). DT-200 Series: Advanced Digital Theodolite. Retrieved from https://content.dicarlotech.com/hubfs/Construction/Topcon%20DT-200/Topcon_DT200_Theodolite_brochure.pdf

Wuhan Huazhiyang Technology Corporation. (2020). Security EOS Electro Optical Systems, Radar Tracking System For Vessel / Aircraft. Retrieved from http://www.eoselectroopticalsystems.com/sale-9967784-security-eos-electro-optical-systems-radar-tracking-system-for-vessel-aircraft.html